High spin spectroscopy in ^{219}Ra: Search for the lower mass boundary of the region of statically octupole-deformed nuclei

T. C. Hensley, P. D. Cottle, Vandana Tripathi, B. Abromeit, M. Anastasiou, L. T. Baby, J. S. Baron, D. Caussyn, R. Dungan, K. W. Kemper, R. S. Lubna, S. L. Miller, N. Rijal, M. A. Riley, S. L. Tabor, P.-L. Tai, and K. Villafana

Phys. Rev. C **96**, 034325 — Published 25 September 2017

DOI: 10.1103/PhysRevC.96.034325

High spin spectroscopy in ^{219}Ra: Search for the lower mass boundary of the region of statically octupole-deformed nuclei

T.C. Hensley, P.D. Cottle, Vandana Tripathi, B. Abromeit, M. Anastasiou, L.T. Baby, J.S. Baron, D. Caussyn, R. Dungan, K.W. Kemper, R.S. Lubna, S.L. Miller, N. Rijal, M.A. Riley, S.L. Tabor, P.-L. Tai, and K. Villafana
Department of Physics, Florida State University, Tallahassee, FL 32306, USA

(Dated: September 14, 2017)

We report the results of a study of rotational bands in ^{219}Ra via the ^{208}Pb(^{14}C,3n) reaction to look for evidence that this nucleus is statically octupole deformed. We add 19 γ rays not previously observed to the level scheme and extend the two most strongly populated alternating parity bands to J=51/2 and 45/2. The magnitude of the energy splitting between the spin-parity doublets in the two bands appears to exclude the possibility that ^{219}Ra has a static octupole deformation.

PACS numbers: May be entered using the `\pacs{#1}` command.

I. INTRODUCTION

It has been known for almost seventy years that many atomic nuclei have shapes that deviate from spherical symmetry in their intrinsic frames [1]. The shapes of nearly all of these deformed nuclei are reflection symmetric relative to a plane perpendicular to the symmetry axis. However, evidence has been accumulating since the mid-1950's that isotopes in two mass regions - one in the light actinide neighborhood of ^{224}Ra [2] and another around ^{144}Ba [3] - might be statically octupole deformed and therefore reflection asymmetric [4].

The larger of these two regions appears to be the one in the vicinity of the $N = 136$ nucleus ^{224}Ra. Evidence for stable octupole deformation has been found in isotopes as heavy as the $N = 138$ isotope ^{229}Pa [4].

In the present work, we address the question of the location of the lower mass boundary of this region of stable octupole deformation. The recent discovery that the lowest negative parity state in the $N = 130$ isotope ^{218}Ra has $J^\pi = 3^-$ [5] definitively excludes the possibility that this nucleus is statically octupole deformed. If ^{218}Ra were statically octupole deformed, the lowest negative parity state would have $J^\pi = 1^-$.

However, there is substantial evidence that isotopes only a few neutrons heavier have stable octupole deformations. Studies of the high spin states of the $N = 133$ isotopes ^{221}Ra [6] and ^{223}Th [7, 8] revealed spectacular parallel $\Delta J = 1$ rotational bands in which states of equal spin and opposite parity - called "parity doublets" - are separated by 60 keV or less. Such parity doublets are characteristic of stable octupole deformation in odd-A or odd-odd isotopes. The rotational bands of the $N = 132$ isotopes ^{220}Ra and ^{222}Th both provide excellent examples of the $\Delta J = 1$ alternating parity bands expected in even-even octupole deformed nuclei [9].

Here we report on an experimental study of rotational bands in the $N = 131$ isotope ^{219}Ra. We investigated whether this isotope is statically octupole deformed by adding 19 γ rays not previously observed to two parallel $\Delta J = 1$ rotational bands and extending these bands to $J = 51/2$ and $45/2$. The separation between the states of equal spin and opposite parity in the two bands vary between 350 and 600 keV, which is much larger than that observed in the octupole deformed $N = 133$ isotones.

II. EXPERIMENTAL DETAILS

The experiment was carried out at the John D. Fox Superconducting Accelerator Laboratory at Florida State University (FSU). A 68 MeV beam of ^{14}C nuclei that was produced by the facility's FN Tandem Van de Graaf accelerator and superconducting linear accelerator booster impinged on a thick (50 mg/cm^2) target of enriched ^{208}Pb. The beam energy was chosen to maximize the cross section for populating the states of interest in ^{219}Ra while keeping the contamination by the $4n$ evaporation channel (^{218}Ra) low.

The γ-ray detector array used for this experiment consisted of seven single crystal HPGe detectors and three clover-style detectors. All of the detectors were Compton-suppressed. The clover detectors were positioned at an angle of 90 degrees relative to the beam axis. The single crystal detectors were arranged at 35 degrees and 145 degrees.

The data were acquired by a Digital Gamma Finder Pixie 16 system. The coincidence and Compton suppression logic was performed by custom firmware in the digitizer. The coincidence condition was set to require two γ-rays arriving together within a time window of 1 μs, and leading edge time stamps were corrected for energy walk. During the experiment, 670 million coincidence events were collected.

The data were analyzed using the RADWARE software package [10]. The level scheme was built using double and triple coincidence events. Having detectors at 90 and 145 degrees allowed an analysis of DCO (Directional Correlation of Oriented States) ratios for some of the stronger transitions, and for this analysis two-dimensional arrays of $\gamma - \gamma$ events for pairs of detectors at different angles were produced.

III. EXPERIMENTAL RESULTS

The level scheme determined in the present study is shown in Figure 1, and details regarding the γ rays measured are listed in Table I. The level scheme is built upon the low-lying structure determined in a conversion electron measurement by Riley *et al.* [11] and the high-spin structure determined by Wieland *et al.* [12]. The γ rays and levels added to the level scheme in the present work are shown in red in Figure 1.

The alternating parity structure of the rotational bands provides a source of confidence in extending the bands to higher spin since the energies of two crossover $E1$ transitions should add up to the energy of each in-band $E2$ transition. Figure 2 shows a segment of the spectrum gated on the 477 keV γ ray, which was one of the two highest-lying $E2$ transitions in Band I in the level scheme given in Ref. [12]. The spectrum shows strong candidates for higher-lying $E2$ transitions at 477 keV (which would be a doublet), 501 keV, 504 keV, 511 keV, and 520 keV. Figure 3 then shows two gated spectra that provide evidence for crossover $E1$ transitions that would interleave with these "new"

$E2$ transitions. The top panel of Figure 3 is a segment of the spectrum gated on the 504 keV γ ray. The spectrum shows several previously-known transitions in Band 1 (187, 205, 235 and 261 keV) as well as two new crossover $E1$ transitions (249 and 270 keV). The bottom panel of Figure 3 illustrates a segment of a spectrum consisting of the sum of spectra gated on the 228, 249, 270, 276, 477 and 504 keV γ rays. This provides evidence for the existence of "new" 227, 231, 249 and 270 $E1$ crossover transitions near the top of Band I. Altogether, there is strong evidence for new states in Band I at 3043.1, 3271.0, 3520.0, 3790.7 and 4021.7 keV. In addition, we tentatively place a state at 4321.9 keV.

The search for new γ rays and states in Band II was similar to that in Band I. The top panel of Figure 4 shows a segment of a spectrum consisting of the sum of spectra gated on the 100 keV, 129 keV, 249 keV, 300 keV, 307 keV, 312 keV, 320 keV, 324 keV, 333 keV, 387 keV, 412 keV and 458 keV transitions. This spectrum shows candidates for $E1$ and $E2$ transitions in this band at energies above 300 keV. The bottom panel is gated on the 435 keV transition, which was the highest $E2$ transition in Band II of the level scheme given in Ref. [12]. It provides additional support for the identification of new $E1$ and $E2$ transitions in Band II.

There are several more $E1$ transitions in Band II at particularly low energies - below 150 keV. These transitions appear in the segment of the spectrum gated on the 306 keV transition shown in Figure 5.

DCO ratios were extracted for fourteen γ rays in Band I, including thirteen that were previously known and one (504 keV) that was not. The ratios were extracted by gating on the 205 keV γ-ray, which has a pure $E1$ multipolariy. The ratio for a particular γ ray is given by

$$R_{DCO} = \frac{I(145\,\mathrm{deg})}{I(90\,\mathrm{deg})}, \tag{1}$$

where $I(145\,\mathrm{deg})$ is the intensity of the γ ray in the 145 deg detectors when gated on by the 205 keV γ ray in the 90 deg detectors, and $I(90\,\mathrm{deg})$ is the intensity of the γ ray in the 90 deg detectors in a spectrum gated by the 205 keV γ ray in the 145 deg detectors.

The DCO ratios for the stretched $E1$ transitions in Band I cluster around 0.99, while those for the stretched $E2$ transitions cluster near 1.96, as shown in Figure 6. There is a clear distinction between the $E1$ and $E2$ transitions, supporting the assignment of the newly-observed 504 keV transition as an $E2$ transition.

TABLE I: **States and γ-rays observed in the present study.**

Band	E [keV]	J^π	E_γ [keV]	I_γ
I	251.2	$15/2^+$	234.6(5)	100(0)
	512.4	$17/2^-$	261.2(6)	29(1)
	545.9	$19/2^+$	294.8(5)	95(3)
	751.0	$21/2^-$	205.1(5)	88(3)
			238.6(8)	5.6(2)
	893.1	$23/2^+$	142.1(5)	45(2)
			347.2(6)	30(1)
	1053.3	$25/2^-$	160.2(5)	61(2)
			302.3(6)	12(1)
	1287.9	$27/2^+$	234.6(5)	41(1)
			394.8(6)	11(1)
	1411.1	$29/2^-$	123.2(6)	31(1)
			357.8(6)	33(1)
	1701.2	$31/2^+$	290.1(6)	34(1)
			413.2(7)	4.8(3)
	1833.0	$33/2^-$	131.9(6)	14(1)
			422.0(6)	25(1)
	2128.8	$35/2^+$	295.7(6)	18(1)
			427.6(8)	3.9(2)
	2289.2	$37/2^-$	160.4(8)	2.3(2)
			456.2(6)	15(1)
	2578.8	$39/2^+$	289.6(7)	9.3(4)
			450.1(8)	3.1(2)
	2766.9	$41/2^-$	188.1(8)	2.7(1)
			477.7(7)	7.1(3)
	3043.1	$43/2^+$	276.2(8)	2.5(1)
			464.2(8)	2.1(1)

Continued on next page

TABLE I – continued from previous page

Band	E [keV]	J^{π}	E_{γ} [keV]	I_{γ}
	3271.0	$45/2^{-}$	227.9(9)	1.3(1)
			504.1(8)	2.9(2)
	3520.0	$47/2^{+}$	249.0(8)	2.2(1)
			477.0(8)	2.1(2)
	3790.7	$49/2^{-}$	270.7(9)	1.0(1)
			519.2(10)	0.5(1)
	4021.7	$51/2^{+}$	231.1(8)	2.7(1)
			501.7(9)	1.3(1)
	4321.9	$53/2^{-}$	300.2(9)	1.6(1)
			531.2(1)	0.13(7)
II	475.2	$13/2^{+}$	361.6(8)	3.2(8)
			458.8(8)	2.1(5)
	604.3	$15/2^{-}$	128.9(7)	6.4(4)
			353.1(9)	1.9(2)
	853.7	$17/2^{+}$	249.4(8)	2.9(2)
			378.3(9)	1.0(1)
	937.8	$19/2^{-}$	84.1(6)	14(1)
			333.5(7)	5.7(3)
			425.4(9)	1.6(2)
	1244.4	$21/2^{+}$	306.6(9)	1.2(2)
			390.7(10)	0.3(1)
	1324.8	$23/2^{-}$	80.4(9)	1.1(1)
			387.0(7)	5.5(3)
			573.8(8)	2.5(2)
	1636.7	$25/2^{+}$	311.9(8)	2.1(2)
			392.4(9)	0.9(1)
	1737.3	$27/2^{-}$	100.6(8)	2.6(1)
			412.5(7)	4.4(3)
			684.0(8)	3.0(2)
	2036.4	$29/2^{+}$	299.1(8)	3.1(2)
			399.7(10)	0.6(1)
	2151.0	$31/2^{-}$	114.6(9)	0.9(1)
			413.7(7)	6.7(3)
			740.0(9)	1.9(2)
	2458.2	$33/2^{+}$	307.1(8)	1.9(2)
			421.7(8)	2.4(2)
	2566.4	$35/2^{-}$	108.2(9)	1.0(1)
			415.4(8)	3.8(2)
			733.3(8)	2.2(2)
	2886.3	$37/2^{+}$	319.9(9)	1.5(1)
			428.1(9)	1.1(1)
	3001.1	$39/2^{-}$	114.8(10)	0.6(1)
			434.7(8)	2.1(2)
			711.9(9)	1.4(1)
	3318.7	$41/2^{+}$	317.6(9)	0.7(1)
			432.5(10)	0.4(1)
	3449.7	$43/2^{-}$	131.0(8)	2.5(1)
			448.6(8)	2.0(1)
			682.3(10)	0.4(1)
	3774.1	$45/2^{+}$	324.3(10)	0.3(1)
			455.3(8)	2.6(2)
	3912.2	$47/2^{-}$	138.2(10)	0.8(1)
			462.5(1)	0.6(1)
III	554.5	$13/2^{+}$	537.9(6)	10(1)
	778.7	$15/2^{-}$	224.2(10)	0.4(1)
	875.8	$17/2^{+}$	97.1(10)	0.4(1)
			321.3(10)	0.4(1)
			624.6(7)	2.5(3)
	1130.0	$19/2^{-}$	254.2(9)	0.9(1)
			351.3(9)	0.4(1)

Continued on next page

TABLE I – continued from previous page

Band	E [keV]	J^π	E_γ [keV]	I_γ
	1256.5	$21/2^+$	126.5(9)	0.8(1)
			380.7(9)	1.0(1)
			710.6(8)	1.0(1)
	1503.2	$23/2^-$	246.7(9)	0.9(1)
			373.2(10)	0.2(1)
	1669.9	$25/2^+$	166.7(10)	0.6(1)
			413.4(10)	0.7(2)
			776.8(10)	0.2(1)
	1931.4	$27/2^-$	261.5(7)	1.6(2)
			428.1(10)	0.2(1)

IV. IS ^{219}Ra STATICALLY OCTUPOLE DEFORMED?

The $N = 133$ isotones ^{221}Ra and ^{223}Th provide spectacular examples of parity doublet rotational bands - parallel alternating parity $\Delta J = 1$ rotational bands in which states of equal spin and opposite parity are nearly degenerate [6–8]. Figure 7 plots the splitting between parity doublet members in the $N = 133$ Ra and Th isotones as well as between the two main rotational bands in ^{219}Ra and between the two corresponding bands in the $N = 131$ isotone ^{221}Th [13]. The situation in the $N = 131$ isotones is clearly different from that in the $N = 133$ isotones.

The details of the plot in Figure 7 are important. For ^{221}Ra, the graph shows the difference in energy between the state of a given spin in the band labeled with the simplex quantum number s as $s = -i$ and the state of the same spin in the band labeled as $s = +i$ in Ref. [6]. For ^{223}Th, the energy splitting shown is the difference between the lower energy band labeled as $s = -i$ and the band labeled as $s = +i$ in Ref. [8]. The key feature in both cases is that the splitting is close to zero for the entire observed spin range.

The quantity plotted for ^{221}Th is the difference between the states in the alternating parity sequence labeled in Ref. [13] as "(b1)" and "(b2)" and the states of identical spin and opposite parity in the alternating parity band labeled "(a)". This difference stays in the range 400-500 keV, which is much larger than that expected for a nucleus that has a static octupole deformation.

The plotted values for ^{219}Ra are the differences between the energies of states in Band II and the states of equal spin and opposite parity in Band I. The present results extend nine units higher in spin than the ^{221}Th result.

In their experimental study of band structure in ^{221}Th, Tandel *et al.* [14] asserted that the large splitting between simplex partner candidates in the $N = 131$ isotones ^{219}Ra and ^{221}Th could be explained if the odd neutron is located in a $K = 1/2$ orbit in a deformed reflection asymmetric field, as proposed by Leander and Chen [15]. In such a scenario, a large Coriolis interaction would affect the band structure and would account for larger splitting in the parity doublets. Such an effect has been observed in the $K = 1/2$ bands of ^{227}Th [16]. The Coriolis interaction could also account for a $7/2^+$ ground state spin and parity in ^{219}Ra, which is one of the two possibilities allowed by the experimental results on the ground state of this nucleus (the other being $11/2^+$).

However, the calculations of ^{219}Ra given by Leander and Chen do not reproduce the size of the parity splitting in this nucleus. They predicted $11/2^+$ and $11/2^-$ states at 197 and 333 keV, respectively, giving a parity splitting of 136 keV. In addition, Leander and Chen predicted splitting of 172 keV between the $13/2^+$ state at 408 keV and the $13/2^-$ state at 580 keV. The lowest spin parity doublet we observe in the present experiment is at $J = 15/2$, and the splitting is 353 keV - considerably larger than the values that Leander and Chen predict for $J = 11/2$ and $13/2$. Therefore, in the absence of further calculations we conclude that it is unlikely that the Coriolis interaction arising from the odd neutron occupying a $K = 1/2$ orbit in a reflection asymmetric field can account for the band structure reported here. Clearly, it is imperative that updated theoretical calculations of the parity splitting be performed - and that they be extended to higher spins.

Even if ^{219}Ra is not stably octupole deformed in its ground state, it is possible that it becomes octupole deformed at a sufficiently high angular frequency. Tsvetkov, Kvasil and Nazmitdinov predicted [17] that a static octupole deformation would stablize in ^{219}Ra at a rotational frequency of 200 keV. In ^{219}Ra, that rotational frequency corresponds to a spin near 27/2. Figure 7 shows that the relationship between the two main bands does not significantly change at that spin. Therefore, we conclude that ^{219}Ra remains reflection symmetric throughout the spin range observed here - up to $J = 47/2$.

On the basis of their study of the low spin structure of ^{219}Ra, Riley *et al.* [11] set out two possibilities for the structure of this nucleus. The first was that it has a static octupole deformation with the odd neutron strongly

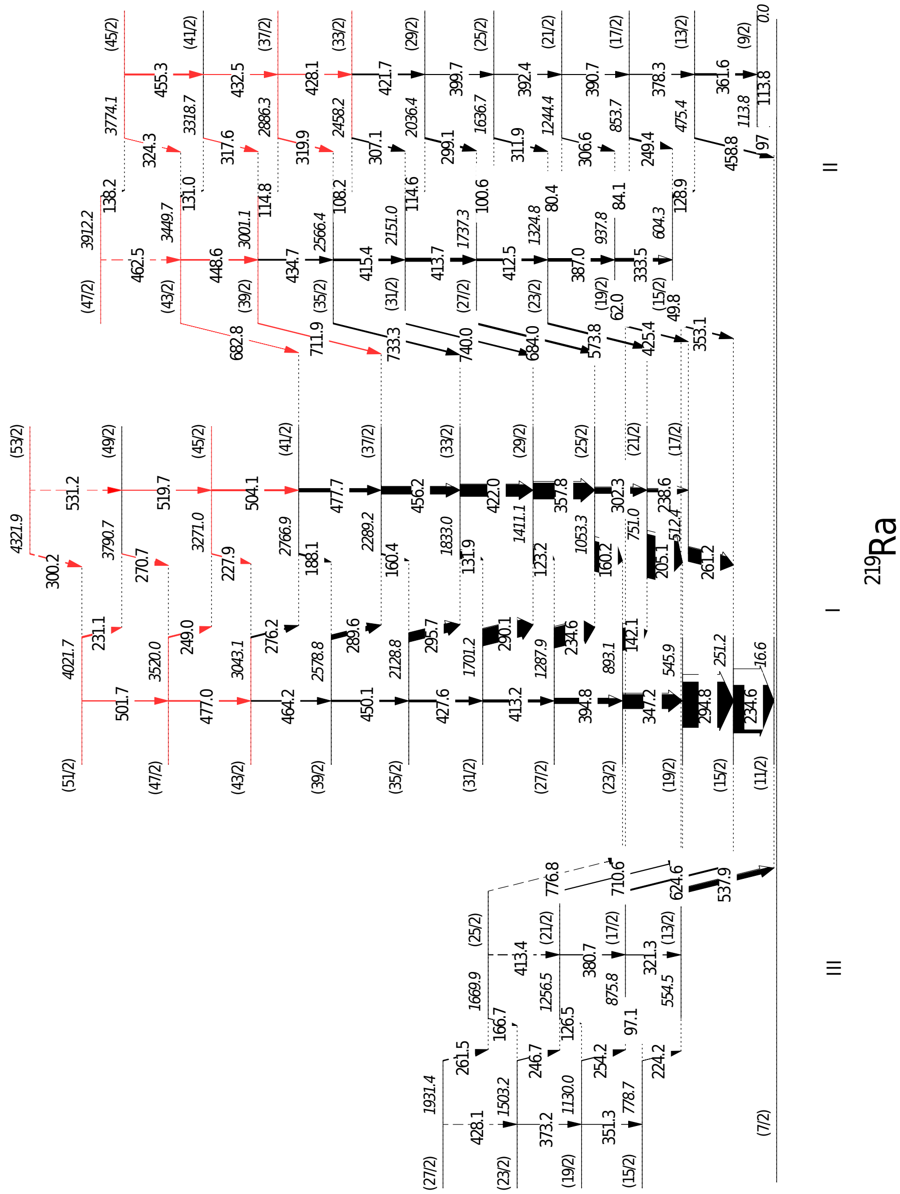

FIG. 1. Level scheme of ^{219}Ra determined in the present work. The states and transitions drawn in red were not observed in previous studies.

coupled to the core. The second possibility was that ^{219}Ra is a transitional nucleus in which the coupling between the odd neutron and the core has an "intermediate" nature between the weak and strong coupling limits. Given the present results, we conclude that the latter possibility is much more likely.

V. SUMMARY

We measured high spin states of ^{219}Ra using the ^{208}Pb(^{14}C,3n) reaction and added 19 γ rays to the level scheme, extending the two most strongly populated alternating parity bands to J=51/2 and 45/2.

The large energy splitting between the two candidates for simplex partner bands is best explained by assuming that ^{219}Ra is a transitional nucleus without a stable octupole deformation and in which the low-lying structure is the result of an intermediate strength coupling between the odd neutron and the core. The particle-core calculations performed

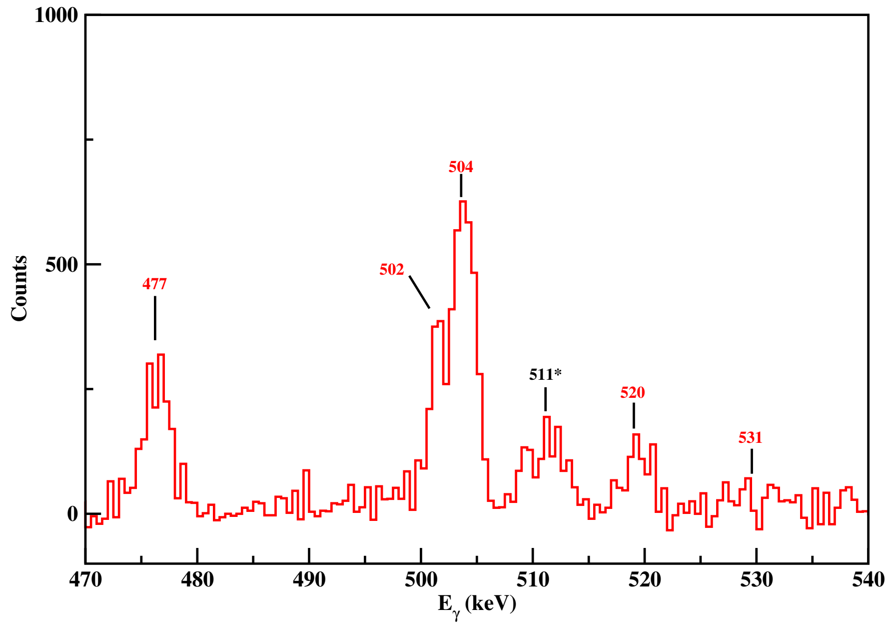

FIG. 2. Evidence for new $E2$ transitions in Band 1. Spectrum is gated on the 477 keV γ ray, which is a doublet. The peaks labeled in red were not observed in previous studies.

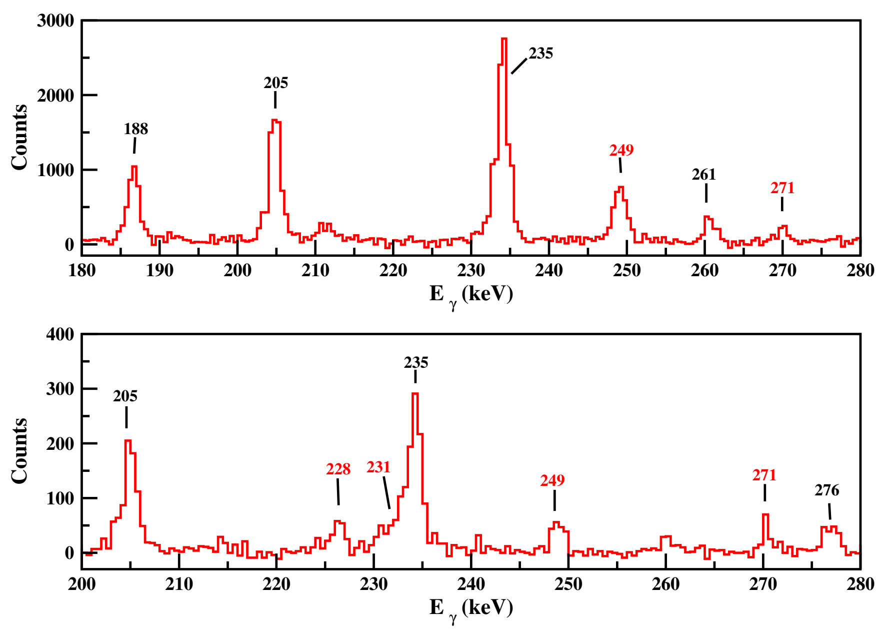

FIG. 3. Evidence for new $E1$ transitions in Band 1. The upper frame is gated on the 504 keV transition. The lower frame is the sum of spectra gated on the 276, 477, 228, 249, 504, and 270 keV transitions. The peaks labeled in red were not observed in previous studies.

by Leander and Chen [15] that assume a reflection asymmetric core, the occupation of the odd neutron in a $K = 1/2$ orbital and a resulting strong Coriolis effect on the band structure do not appear to reproduce the magnitude of the energy splitting between the two rotational bands.

Therefore, we conclude that ^{220}Ra is the lightest radium isotope that is statically octupole deformed.

ACKNOWLEDGMENTS

This work was supported by the National Science Foundation under Grant number 14-01574.

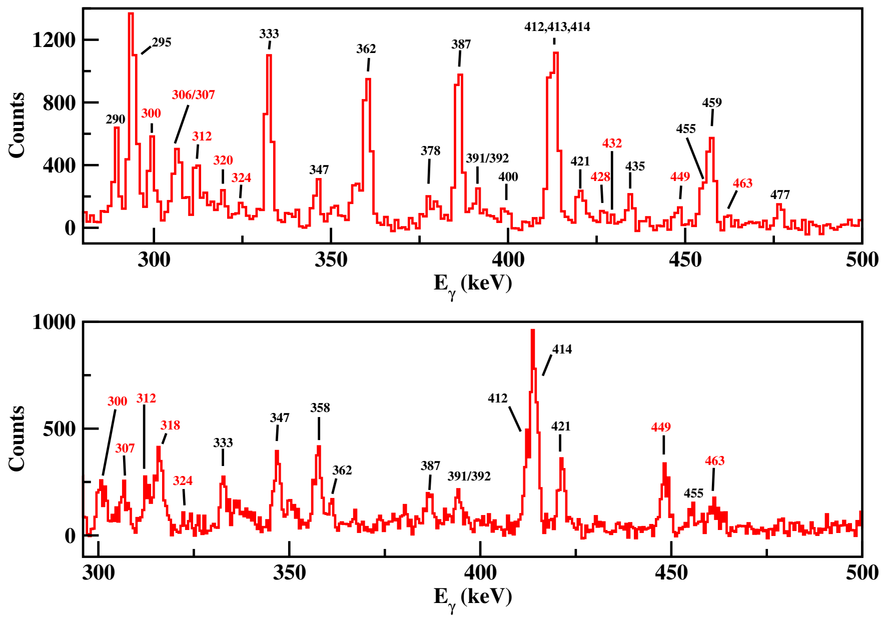

FIG. 4. Evidence for new $E2$ transitions in Band 2. The upper panel shows the sum of spectra gated on 458,129, 333, 249,387,307,412, 312, 100, 300, 320, and 324 keV γ rays. The 477 keV peak seen in this panel is a contaminant from Band 1. The lower panel displays the spectrum gated on the 435 keV γ ray. The peaks labeled in red were not observed in previous studies.

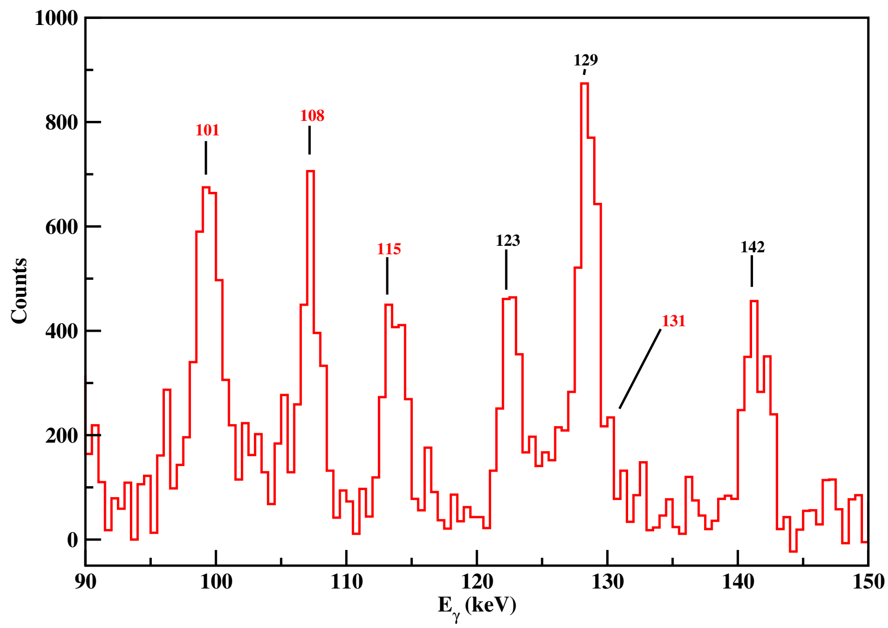

FIG. 5. Evidence for new $E1$ transitions in Band 2 from the spectrum gated on the 306 keV γ ray. The peaks labeled in red were not observed in previous studies.

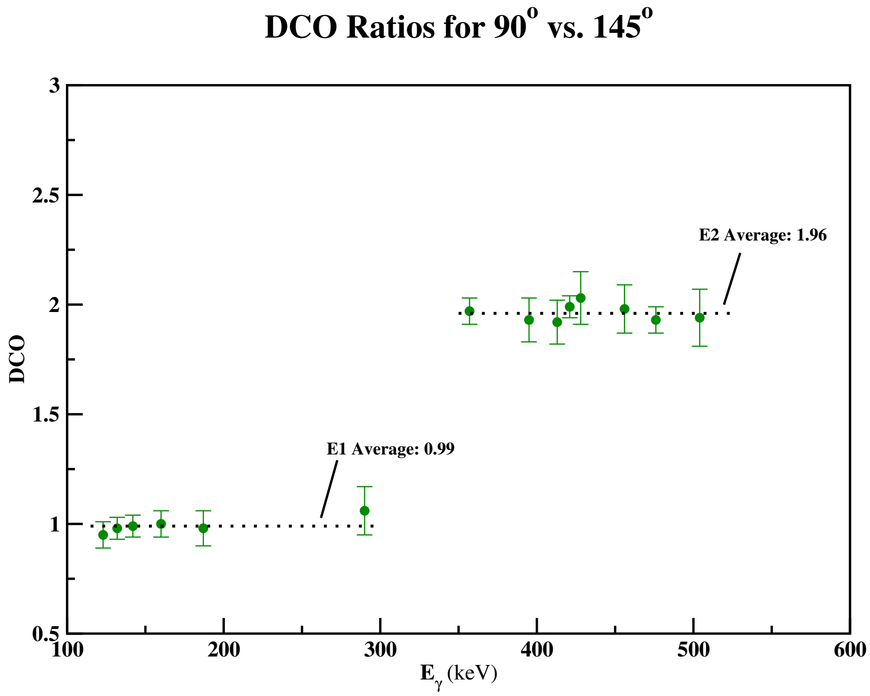

FIG. 6. DCO ratios for transitions in Band I, as described in the text.

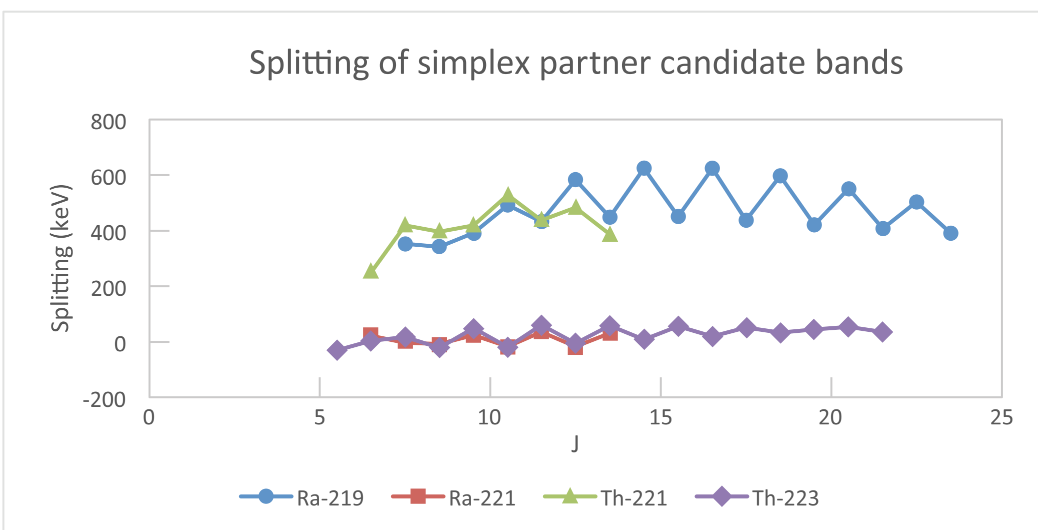

FIG. 7. Energy splitting between candidates for simplex partner bands in ^{219,221}Ra and ^{221,223}Th. Details are given in the text. The data are taken from Refs. [6, 7, 11–13] and the present work.

[1] J. Rainwater, Phys. Rev. **79**, 432 (1950).
[2] L. P. Gaffney, P. A. Butler, M. Scheck, A. B. Hayes, F. Wenander, M. Albers, B. Bastin, C. Bauer, A. Blazhev, S. Bonig, N. Bree, J. Cederkall, T. Chupp, D. Cline, T. E. Cocolios, T. Davinson, H. De Witte, J. Diriken, T. Grahn, A. Herzan, M. Huyse, D. G. Jenkins, D. T. Joss, N. Kesteloot, J. Konki, M. Kowalczyk, T. Kroll, E. Kwan, R. Lutter, K. Moschner, P. Napiorkowski, J. Pakarinen, M. Pfeiffer, D. Radeck, P. Reiter, K. Reynders, S. V. Rigby, L. M. Robledo, M. Rudigier, S. Sambi, M. Seidlitz, B. Siebeck, T. Stora, P. Thoele, P. Van Duppen, M. J. Vermeulen, M. von Schmid, D. Voulot, N. Warr, K. Wimmer, K. Wrzosek-Lipska, C. Y. Wu, and M. Zielinska, Nature **497**, 199 (2013).
[3] B. Bucher, S. Zhu, C. Y. Wu, R. V. F. Janssens, D. Cline, A. B. Hayes, M. Albers, A. D. Ayangeakaa, P. A. Butler, C. M. Campbell, M. P. Carpenter, C. J. Chiara, J. A. Clark, H. L. Crawford, M. Cromaz, H. M. David, C. Dickerson, E. T. Gregor, J. Harker, C. R. Hoffman, B. P. Kay, F. G. Kondev, A. Korichi, T. Lauritsen, A. O. Macchiavelli, R. C. Pardo, A. Richard, M. A. Riley, G. Savard, M. Scheck, D. Seweryniak, M. K. Smith, R. Vondrasek, and A. Wiens, Phys. Rev. Lett. **116**, 112503 (2016).
[4] P. A. Butler and W. Nazarewicz, Rev. Mod. Phys. **68**, 349 (1996).
[5] E. Parr, J. F. Smith, P. T. Greenlees, M. Smolen, P. Papadakis, K. Auranen, R. Chapman, D. M. Cullen, T. Grahn, L. Grocutt, A. Herzáň, R.-D. Herzberg, D. Hodge, U. Jakobsson, R. Julin, S. Juutinen, J. Konki, M. Leino, C. McPeake, D. Mengoni, A. K. Mistry, K. F. Mulholland, G. G. O'Neill, J. Pakarinen, J. Partanen, P. Peura, P. Rahkila, P. Ruotsalainen, M. Sandzelius, J. Sarén, M. Scheck, C. Scholey, J. Sorri, S. Stolze, M. J. Taylor, and J. Uusitalo, Phys. Rev. C **94**, 014307 (2016).
[6] J. Fernandez-Niello, C. Mittag, F. Riess, E. Ruchowska, and M. Stallknecht, Nuclear Physics A **531**, 164 (1991).
[7] M. Dahlinger, E. Kankeleit, D. Habs, D. Schwalm, B. Schwartz, R. Simon, J. D. Burrows, and P. A. Butler, Nuclear Physics A **484**, 337 (1988).
[8] G. Maquart, L. Augey, L. Chaix, I. Companis, C. Ducoin, J. Dudouet, D. Guinet, G. Lehaut, C. Mancuso, N. Redon, O. Stézowski, A. Vancraeyenest, A. Astier, F. Azaiez, S. Courtin, D. Curien, I. Deloncle, O. Dorvaux, G. Duchêne, B. Gall, T. Grahn, P. Greenlees, A. Herzan, K. Hauschild, U. Jakobsson, P. Jones, R. Julin, S. Juutinen, S. Ketelhut, M. Leino, A. Lopez-Martens, P. Nieminen, P. Petkov, P. Peura, M.-G. Porquet, P. Rahkila, S. Rinta-Antila, M. Rousseau, P. Ruotsalainen, M. Sandzelius, J. Sarén, C. Scholey, J. Sorri, S. Stolze, and J. Uusitalo, Phys. Rev. C **95**, 034304 (2017).
[9] J. F. Smith, J. F. C. Cocks, N. Schulz, M. Aïche, M. Bentaleb, P. A. Butler, F. Hannachi, G. D. Jones, P. M. Jones, R. Julin, S. Juutinen, R. Kulessa, E. Lubkiewicz, A. Płochocki, F. Riess, E. Ruchowska, A. Savelius, J. C. Sens, J. Simpson, and E. Wolf, Phys. Rev. Lett. **75**, 1050 (1995).
[10] D. Radford, Nuclear Instruments and Methods in Physics Research Section A: Accelerators, Spectrometers, Detectors and Associated Equipment **361**, 297 (1995).
[11] L. A. Riley, P. D. Cottle, M. Fauerbach, V. S. Griffin, B. N. Guy, K. W. Kemper, G. S. Rajbaidya, and O. J. Tekyi-Mensah, Phys. Rev. C **62**, 021301 (2000).
[12] M. Wieland, J. Fernández Niello, F. Riess, M. Aïche, A. Chevallier, J. Chevallier, N. Schulz, J. C. Sens, C. Briançon, R. Kulessa, and E. Ruchowska, Phys. Rev. C **45**, 1035 (1992).
[13] W. Reviol, R. V. F. Janssens, S. Frauendorf, D. G. Sarantites, M. P. Carpenter, X. Chen, C. J. Chiara, D. J. Hartley, K. Hauschild, T. Lauritsen, A. Lopez-Martens, M. Montero, O. L. Pechenaya, D. Seweryniak, J. B. Snyder, and S. Zhu, Phys. Rev. C **90**, 044318 (2014).
[14] S. K. Tandel, M. Hemalatha, A. Y. Deo, S. B. Patel, R. Palit, T. Trivedi, J. Sethi, S. Saha, D. C. Biswas, and S. Mukhopadhyay, Phys. Rev. C **87**, 034319 (2013).
[15] G. A. Leander and Y. S. Chen, Phys. Rev. C **37**, 2744 (1988).
[16] N. J. Hammond, G. D. Jones, P. A. Butler, R. D. Humphreys, P. T. Greenlees, P. M. Jones, R. Julin, S. Juutinen, A. Keenan, H. Kettunen, P. Kuusiniemi, M. Leino, M. Muikku, P. Nieminen, P. Rahkila, J. Uusitalo, and S. V. Khlebnikov, Phys. Rev. C **65**, 064315 (2002).
[17] A. Tsvetkov, J. Kvasil, and R. G. Nazmitdinov, Journal of Physics G: Nuclear and Particle Physics **28**, 2187 (2002).